Prominent neurodegeneration and increased plaque formation in complement-inhibited Alzheimer's mice

Tony Wyss-Coray*†‡, Fengrong Yan*, Amy Hsiu-Ti Lin*, John D. Lambris§, Jessy J. Alexander¶, Richard J. Quigg¶, and Eliezer Masliah‖

*Gladstone Institute of Neurological Disease and †Department of Neurology, University of California, San Francisco, CA 94141; §Department of Pathology and Laboratory Medicine, University of Pennsylvania, Philadelphia, PA 19104; ¶Department of Medicine, Section of Nephrology, University of Chicago, Chicago, IL 60637; and ‖Departments of Neurosciences and Pathology, University of California at San Diego, La Jolla, CA 92093

Communicated by Robert W. Mahley, The J. David Gladstone Institutes, San Francisco, CA, June 11, 2002 (received for review April 16, 2002)

Abnormal accumulation of β-amyloid (Aβ) in Alzheimer's disease (AD) is associated with prominent brain inflammation. Whereas earlier studies concluded that this inflammation is detrimental, more recent animal data suggest that at least some inflammatory processes may be beneficial and promote Aβ clearance. Consistent with these observations, overproduction of transforming growth factor (TGF)-β1 resulted in a vigorous microglial activation that was accompanied by at least a 50% reduction in Aβ accumulation in human amyloid precursor protein (hAPP) transgenic mice. In a search for inflammatory mediators associated with this reduced pathology, we found that brain levels of C3, the central component of complement and a key inflammatory protein activated in AD, were markedly higher in hAPP/TGF-β1 mice than in hAPP mice. To assess the importance of complement in the pathogenesis of AD-like disease in mice, we inhibited C3 activation by expressing soluble complement receptor-related protein y (sCrry), a complement inhibitor, in the brains of hAPP mice. Aβ deposition was 2- to 3-fold higher in 1-year-old hAPP/sCrry mice than in age-matched hAPP mice and was accompanied by a prominent accumulation of degenerating neurons. These results indicate that complement activation products can protect against Aβ-induced neurotoxicity and may reduce the accumulation or promote the clearance of amyloid and degenerating neurons. These findings provide evidence for a role of complement and innate immune responses in AD-like disease in mice and support the concept that certain inflammatory defense mechanisms in the brain may be beneficial in neurodegenerative disease.

Alzheimer's disease (AD) causes an incurable age-dependent dementia that afflicts millions of people worldwide. The disease is characterized by the accumulation of extracellular Aβ deposits in amyloid plaques and cerebral blood vessels and by the formation of tangles inside neurons. These lesions are associated with progressive neurodegeneration and activation of inflammatory pathways in the brain (1–3). Although the cause of the disease is still unknown, there is strong evidence that accumulation of the 40- to 42-aa Aβ peptide is key to disease pathogenesis (4, 5). Why this naturally occurring peptide accumulates in the brain is still not clear for most cases with AD. Possible mechanisms include increased synthesis, a higher tendency to aggregate, and impaired clearance. Inhibiting the synthesis or aggregation of Aβ or increasing its clearance may reduce the detrimental effects of this peptide and consequently improve cognitive functions in patients.

Indeed, recent studies showed that increased clearance of Aβ can improve cognitive function in mouse models of AD (6, 7). Clearance in these experiments was achieved by immunizing mice with synthetic Aβ, which can prevent or reduce Aβ accumulation (8). Reduced Aβ accumulation was accompanied by a prominent inflammatory reaction, and activated microglia have been suggested to remove Aβ by antibody-dependent, Fc receptor-mediated phagocytosis (8–10). Activated microglia can also internalize Aβ injected into the rat brain (11), and prominent microgliosis is associated with reduced Aβ accumulation in APP mice treated with NO-flurbiprofen (12). We have shown that microglial activation is associated with reduced cerebral Aβ accumulation and neurodegeneration in hAPP mice overproducing TGF-β1 and that TGF-β1 increases the clearance of Aβ in cultured BV-2 microglial cells (13). How microglia might naturally clear Aβ is not known.

The observation that increased immune or inflammatory reactions and microglial activation are associated with less AD-type pathology and improved cognitive function in APP mice is of major interest. Most studies have argued that the prominent increase in inflammatory markers in the AD brain indicates a detrimental role of inflammation (1, 3). For example, activated microglia have been suggested to release neurotoxins (14), and the colocalization of complement activation products and the membrane attack complex (MAC) on amyloid plaques and degenerating neurons was hypothesized to indicate a pathogenic role of complement in neurodegeneration (1, 3).

The complement system is a key initiator of inflammation (15) and may be of particular importance in AD. Complement activation stimulates innate inflammatory cells and adaptive immune responses, promotes phagocytosis, and facilitates complement-mediated lysis by the MAC (16). Although 80–90% of all complement proteins are produced in the liver and are present at high levels in the serum, glial cells and neurons in the central nervous system (CNS) can produce most components of this complex cascade, and their production is increased in AD (1, 3, 17–19). Aggregated Aβ activates the complement system *in vitro* through the classical pathway by binding Clq and through the alternative pathway by binding C3b (20–24). Both pathways lead to the formation of multiprotein enzyme complexes, the C3 convertases, which cleave C3 into C3a and C3b (25). C3a is released in the fluid phase and is involved in the chemotaxis of phagocytes. C3b binds covalently to acceptor molecules and tags cells in a process called opsonization, leading to further activation of the complement cascade in the lytic pathway, which culminates in the formation of the MAC and cell lysis. Alternatively, C3b deposition mediates phagocytosis through complement receptors on specialized cells (15). Cells are protected from spontaneous complement activation and self-attack by a number of soluble or membrane-bound complement regulatory proteins. One such protein, found in mice, is complement receptor-related protein y (Crry), which is a potent inhibitor of complement C3 convertases. Crry is a rodent-specific functional homologue of two human regulators of complement activation (membrane cofactor protein and decay-accelerating factor) and

Abbreviations: AD, Alzheimer's disease; CNS, central nervous system; hAPP, human amyloid precursor protein; MAC, membrane attack complex; sCrry, soluble complement receptor-related protein Y; TGF-β1, transforming growth factor-β1.

‡To whom reprint requests should be addressed. E-mail: twysscoray@gladstone.ucsf.edu.

NEUROBIOLOGY

inhibits complement activation and C3 deposition by both the classical and the alternative pathways (26, 27).

The pathophysiological role of complement activation in AD is unknown. In this study, we used a transgenic approach to test the role of complement in the development of AD-like pathology in mice expressing hAPP with or without a soluble form of Crry in the brain.

Materials and Methods

Transgenic Mice. Mice expressing hAPP under control of the platelet-derived growth factor B chain promoter (ref. 28; line J20, courtesy of L. Mucke, Gladstone Institute of Neurological Disease) on the C57BL/6 genetic background were generated with an alternatively spliced minigene that encodes hAPP695, hAPP751, and hAPP770 bearing the amyloidogenic K670M/N671L and V717F mutations, which have been linked to early onset familial AD. C3 knockout mice used as controls for immunohistochemical staining were kindly provided by H. Molina, Washington University, St. Louis. Low-expressor TGF-β1 transgenic mice (13) on a C57BL/6 genetic background express a bioactive form of porcine TGF-β1 in astrocytes under control of glial fibrillary acidic protein regulatory sequences. Crry transgenic mice (27) on the CD1 genetic background express a truncated soluble form of Crry (sCrry) under control of the metallothionein promoter. To increase transcription from the metallothionein promoter (27), all mice derived from crosses of hAPP with sCrry mice used in this study were fed with $ZnSO_4$ (25 mM) in their drinking water throughout life. Littermates served as controls for heterozygous transgenic mice in all experiments.

Tissue Preparation and Immunohistochemistry. Mice were anesthetized with chloral hydrate before transcardiac saline perfusion, and brains were removed and fixed for 48 h in phosphate-buffered 4% paraformaldehyde for neuropathological analysis. Sagittal brain sections (40 μm thick) were cut with a vibratome and stained with thioflavin S (13) or the following primary antibodies: rabbit anti-human C3d (1:200; Dako); 3D6 mouse anti-human Aβ_{1-5} (3 μg/ml; Elan Pharmaceuticals, South San Francisco); 8E5 mouse anti-human APP (2 μg/ml; Elan Pharmaceuticals; ref. 29); rabbit anti-GFAP (1:1000; Dako), rat anti-mouse F4/80 (1:60; Serotec); or AT8 mouse antiphosphorylated tau (1:500; Biosource International, Camarillo, CA). Primary antibody staining was revealed with fluorescently tagged secondary antibodies or with an immunoperoxidase technique (13). Sections were viewed by light or fluorescence microscopy, and digital images were captured with a Zeiss Axiocam camera. For some experiments, digital images were analyzed with the Bioquant image-analysis system (R & M Biometrics, Nashville) to determine relative areas occupied by immunoreactive material or numbers of stained cells or plaques. For Congo Red staining, vibratome sections were dried overnight on glass slides, stained for 1 h with a 1% aqueous Congo Red solution, and differentiated in a 1% NaOH/ethyl alcohol solution. Sections were viewed under polarized or normal light. Brain sections immunolabeled for microtubule-associated protein (MAP)-2 (a marker for neuronal cell bodies and dendrites) were analyzed with a laser-scanning confocal microscope essentially as described (28). The area occupied by MAP-2-immunoreactive dendrites was quantified and expressed as a percentage of the total image area. The number of neurons in the neocortex or the CA2/CA3 region of the hippocampus was counted on NeuN-immunolabeled brain sections with the Quantimet imaging system and the optical disector approach (30).

Western Blots. Hemibrains were homogenized in triple lysis detergent buffer (50 mM Tris·HCl, pH 8.0/150 mM NaCl/0.1% SDS/1% Nonidet P-40/0.5% sodium deoxycholate and protease inhibitors) or PBS (for C3 detection), incubated for 30 min on ice, and centrifuged at 12,000 $\times$ *g*. Supernatants (80 μg protein per lane) were diluted in lithium dodecyl sulfate sample buffer (Novex, San Diego) and separated under nonreducing conditions on 3–8% Tris-acetate gels (Novex) or under reducing conditions (0.4 M 2-mercaptoethanol/1 mM DTT) on 4–12% Bis-Tris gels (Novex) with 3-(*N*-morpholino)-propanesulfonic acid (Mops) running buffer. After transfer to 0.2 μm nitrocellulose membranes (BA-S 83; Schleicher & Schuell), blots were blocked with 5% nonfat dry milk in PBS and stained with a rabbit anti-mouse C3c antibody (1:500, D. Mastellos, and J.D.L., unpublished data) or a goat anti-mouse C3 antibody (1:500; Cappel, Aurora, OH) or with the hAPP-specific antibody 8E5 (2 μg/ml) and appropriate peroxidase-conjugated secondary antibodies. Blots were developed with ECL chemiluminescence reagents (Amersham Pharmacia) and exposed to autoradiography films. Films were scanned, and the relative intensities of immunoreactive products were quantitated with NIH IMAGE software. For each genotype, four or five mice were analyzed.

RNA Extraction. Total RNA from snap-frozen hemibrains was analyzed by solution hybridization RNase protection assay (13). mRNA levels were quantitated from PhosphorImager readings of probe-specific signals corrected for RNA content/loading errors by normalization to cyclophilin signals. The following ^{32}P-labeled antisense riboprobes were used to identify specific mRNAs: mouse cyclophilin [nucleotides 38–140 (accession no. X52803), Ambion, Austin, TX], human APP [nucleotides 2468–2657 (X06989) of human APP fused with a *Not*I linker to nucleotides 2532–2656 (M24914) of SV40], mouse Crry [nucleotides 567–768 (NM013499)], and mouse C3 [nucleotides 4636–4915 (K02782)].

Aβ ELISA. Snap-frozen hippocampus and neocortex were homogenized in 5 M guanidine buffer, and human total Aβ (Aβ_{1-x}) and Aβ_{1-42} were measured by ELISA (31). A sandwich ELISA consisting of capture antibody 266 (anti-human Aβ_{13-28}) and biotinylated reporter antibody 3D6 (anti-human Aβ_{1-5}) was used to estimate total Aβ levels. Hence, this assay measures levels of Aβ species ranging from amino acid positions 1–28 and longer. Aβ_{1-42} levels were measured with capture antibody 21F12 (anti-human Aβ_{33-42}) and biotinylated detection antibody 3D6. All antibodies were from Elan Pharmaceuticals.

Statistical Analysis. Statistical analyses were performed with STATVIEW 5.0 software (SAS Institute, Cary, NC). For histochemical and immunohistochemical studies, the brain sections were coded, and the codes were not broken until the analyses were complete.

Results

Increased Cerebral C3 Production Is Associated with Reduced Aβ Deposition in Mice. In hAPP/TGF-β1 mice, cerebral levels of C3 mRNA were 5-fold higher than in hAPP mice at 2 months of age and 2-fold higher at 12–15 months (Fig. 1*A*). In contrast, the number of Aβ deposits in hAPP/TGF-β1 mice was 3- to 4-fold lower than in hAPP mice (Fig. 1*B* and ref. 13), and mice with the fewest Aβ deposits had the highest levels of C3 mRNA (data not shown). Notably, this increase in C3 mRNA levels precedes overt pathological changes and Aβ deposition in the brain parenchyma in hAPP/TGF-β1 mice (13). Cerebral overexpression of TGF-β1 also increased expression of C3 protein (Fig. 1*C*).

sCrry Expression in hAPP Mice Results in Increased Aβ Deposition. To determine the role of complement activation in Aβ accumulation and neurodegeneration, we inhibited C3 activation genetically in brains of hAPP mice by expressing the C3 convertase inhibitor Crry under control of the metallothionein promoter

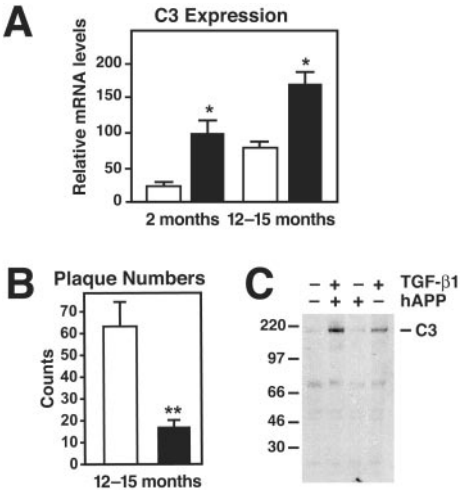

Fig. 1. Increased complement C3 expression in hAPP/TGF-β1 and TGF-β1 transgenic mice. (*A*) Brains from hAPP (white bars) and hAPP/TGF-β1 (black bars) mice at the indicated ages were divided sagitally, and relative C3 mRNA levels were measured by RNase protection assay in one hemibrain. (*B*) In the opposite hemibrain, average numbers of thioflavin S-positive plaques per 40-μm brain section (5–6 sections per mouse; hippocampus plus neocortex) were counted. Values are mean ± SEM from 4–6 mice per group. *, $P < 0.05$; **, $P < 0.001$ by *t* test. (*C*) Western blot analysis of solubilized total brain homogenates from 15-month-old hAPP, hAPP/TGF-β1, TGF-β1, and nontransgenic littermate mice was performed under nonreducing conditions with an anti-C3 (C3c) antibody. The α/β dimer of C3 (185 kDa) is indicated on the right.

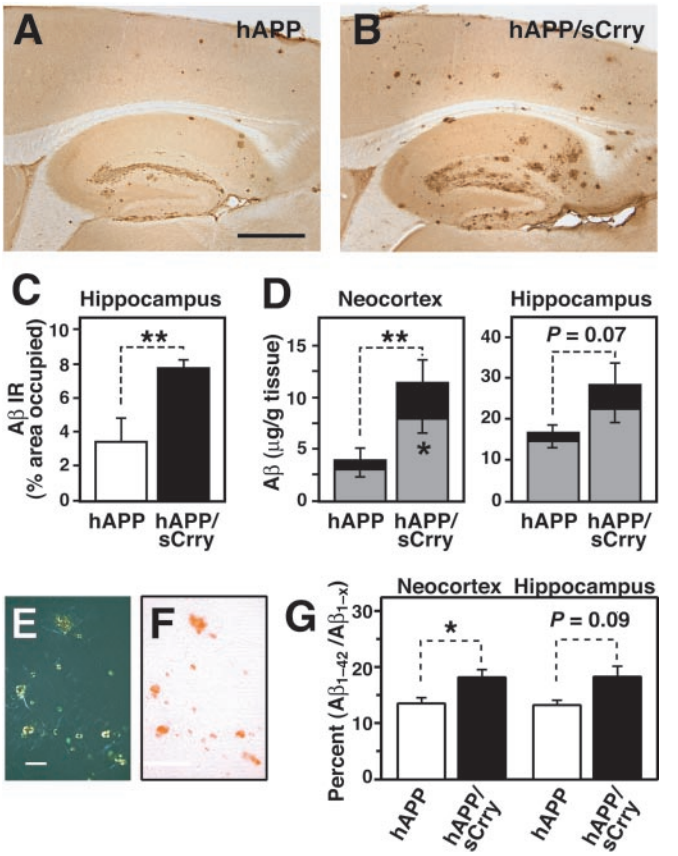

Fig. 2. Increased Aβ accumulation and amyloid formation in hAPP/sCrry mice. (*A–F*) Brains from 10- to 12-month-old hAPP ($n = 6$) and hAPP/sCrry ($n = 8$) mice were dissected and analyzed for Aβ accumulation and amyloid formation. (*A* and *B*) Aβ immunostaining in the hippocampus and neocortex of an hAPP (*A*) and an hAPP/sCrry (*B*) mouse. (*C*) The area occupied by Aβ immunoreactivity was significantly larger in hAPP/sCrry than in hAPP mice. Values are mean ± SEM. **, $P < 0.01$ by *t* test. (*D*) Total Aβ (A$\beta_{1\text{-}x}$, black + gray bars) and Aβ_{1-42} levels (gray bars) in neocortex and hippocampus of hAPP and hAPP/sCrry mice. Values are mean ± SEM. **, $P = 0.028$; *, $P = 0.039$ by *t* test. (*E* and *F*) Congo red staining in the hippocampus of an hAPP/sCrry mouse viewed with crosspolarized filters (*E*) or under normal light (*F*). (*G*) Aβ_{1-42}/A$\beta_{1\text{-}x}$ ratios in neocortex and hippocampus of 3-month-old hAPP/sCrry ($n = 9$; black bars) and hAPP ($n = 8$; white bars) mice as measured by ELISA. Values are mean ± SEM. *, $P < 0.05$ by *t* test. [Scale bars: 250 μm (*A* and *B*), 100 μm (*E* and *F*).]

(27). Whereas Crry is normally expressed in a membrane-bound form in astrocytes, microglia, and neurons (32), the transgenic mice used here also express Crry in a soluble form (sCrry). sCrry has been used successfully to inhibit complement activation in the brain or peripheral organs in transgenic mice (27, 32, 33). Cerebral Crry mRNA levels were 6-fold higher in sCrry and hAPP/sCrry mice than in hAPP and nontransgenic littermate controls, and hAPP expression did not change Crry mRNA levels (data not shown).

At 10–12 months of age, hAPP/sCrry mice showed more Aβ immunostaining than hAPP mice (Fig. 2 *A* and *B*) and a significant increase in hippocampal Aβ-immunoreactive area (Fig. 2*C*). A$\beta_{1\text{-}x}$ and Aβ_{1-42} levels were on average 3-fold higher in the neocortex and almost 2-fold higher in the hippocampus of hAPP/sCrry mice than in hAPP littermate controls (Fig. 2*D*). hAPP/sCrry mice also had significantly more thioflavin S-positive plaques (78.3 ± 8.5 vs. 47.4 ± 6.4; $n = 6$–7 per group, 3–4 sagittal brain sections per case; $P = 0.028$ by Mann–Whitney *U* test) and Congo Red–positive plaques (Fig. 2 *E* and *F* and data not shown) in the hippocampus than hAPP littermate controls. hAPP/sCrry mice had significantly higher Aβ_{1-42}/A$\beta_{1\text{-}x}$ ratios in the neocortex at 3 months of age than hAPP mice, suggesting an effect of sCrry on Aβ turnover and possibly on Aβ_{1-42} clearance (Fig. 2*G*). These results indicate that inhibition of complement results in greater accumulation of Aβ and increases the number of compact amyloid plaques.

Because hAPP mRNA levels were not significantly different between hAPP and hAPP/sCrry mice at 12 months of age (data not shown), it is likely that the changes in Aβ accumulation and deposition were not caused by increased production of APP or Aβ. This is further supported by the observations that hAPP protein levels in brain homogenates (Fig. 3*A*), hAPP immunoreactivity in hippocampal CA neurons (data not shown), and total Aβ levels (A$\beta_{1\text{-}x}$) measured by ELISA in the cortex (data not shown) or hippocampus were similar in 3-month-old hAPP and hAPP/sCrry mice (222 ± 33 vs.224 ± 35 ng/g tissue; $n =$ 8–9 per group). In addition, no significant differences between the four genotypes were observed in levels of full-length C3 in brains of 12-month-old (data not shown) or 3-month-old mice (Fig. 3*B*). One-year-old hAPP, but not hAPP/sCrry, mice showed a trend toward higher hippocampal levels of C3d, a proteolytic activation fragment of C3 (Fig. 3*C*).

sCrry Expression in hAPP Mice Results in Accumulation of Degenerating, Electron-Dense Neurons. At 10–12 months of age, hAPP/sCrry mice had 50% fewer NeuN-positive hippocampal CA3 pyramidal neurons than hAPP mice (Fig. 4 *A* and *B*). Mice with the fewest of these neurons also had the most Aβ immunoreactivity in the hippocampus (Fig. 4*C*). In addition, NeuN-positive cells were significantly less numerous in layers II and III of the neocortex of aged hAPP/sCrry than of nontransgenic littermate control mice (128 ± 18 vs.212 ± 20; mean ± SEM of number of neurons per optical field of 5–8 mice per group; $P <$ 0.05 by Tukey–Kramer test); hAPP, sCrry, and control mice had similar numbers of NeuN-positive cells. In 3-month-old mice, the number of NeuN-positive neurons did not differ among the four

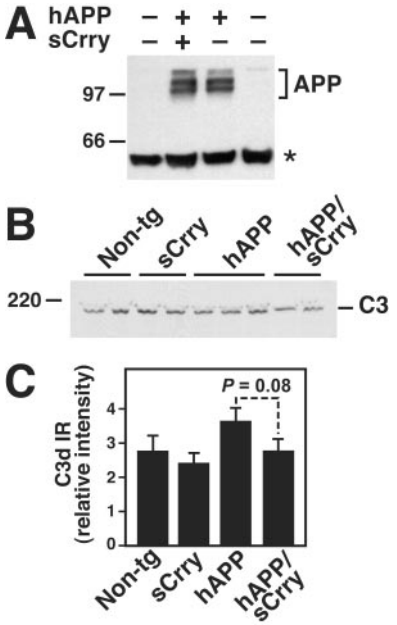

Fig. 3. Transgene and complement expression in hAPP and hAPP/sCrry brains. (*A*) Similar levels of hAPP were detected in hippocampal homogenates from 3-month-old hAPP and hAPP/sCrry mice by Western blot analysis with the 8E5 antibody. APP, hAPP isoforms; asterisk indicates a nonspecific band. (*B*) Similar levels of C3 were detected in hippocampal homogenates from 3-month-old mice of four genotypes by Western blot analysis with an anti-C3 (C3c) antibody. (*C*) Relative C3d immunoreactivity (IR) in the stratum radiatum of the CA3 hippocampal region of 12-month-old mice calculated from four measurements per case. Values are mean ± SEM from three mice per genotype.

genotypes analyzed (data not shown). hAPP/sCrry mice showed also dendritic degeneration in the CA3 subfield as determined by a decrease in MAP-2-immunopositive dendrites (Fig. 4*D*). In addition, hAPP/sCrry mice had more dystrophic neurites than hAPP mice, as demonstrated by staining of brain sections with AT8, an antibody specific for hyperphosphorylated tau (data not shown). Despite this increase in neurodegeneration, microglia were significantly less activated in the cortex of hAPP/sCrry mice than in hAPP mice, and microglia surrounding plaques appeared less activated (Fig. 4 *E–G*).

NeuN stains most differentiated neurons in the adult neocortex (34), but degenerating neurons seem to lose this marker (35). The CA3c subregion showed the greatest loss of NeuN immunostaining in hAPP/sCrry mice and also exhibited atypically intense cresyl violet (data not shown) and toluidine blue staining of shrunken neurons (Fig. 5*B*). Electron microscopy confirmed the presence of degenerating neurons with various degrees of electron density, particularly in the CA3 pyramidal cell layer (Fig. 5 *F* and *G*) and the granule cell layer of the dentate gyrus. The neutrophil in the hippocampus and neocortex showed widespread accumulation of electron-dense neurites and nerve terminals (Fig. 5*E*). hAPP (data not shown) and nontransgenic control brains (Fig. 5 *C* and *D*) did not show such damage.

Discussion

This study demonstrates that expression of a complement inhibitor increased AD-like pathology, including amyloid deposition and neurodegeneration, in hAPP mice, whereas increased complement C3 production was associated with reduced Aβ deposition in hAPP/TGF-β1 transgenic mice. Thus, complement activation products may protect against Aβ-induced toxicity and reduce the accumulation or promote the clearance of

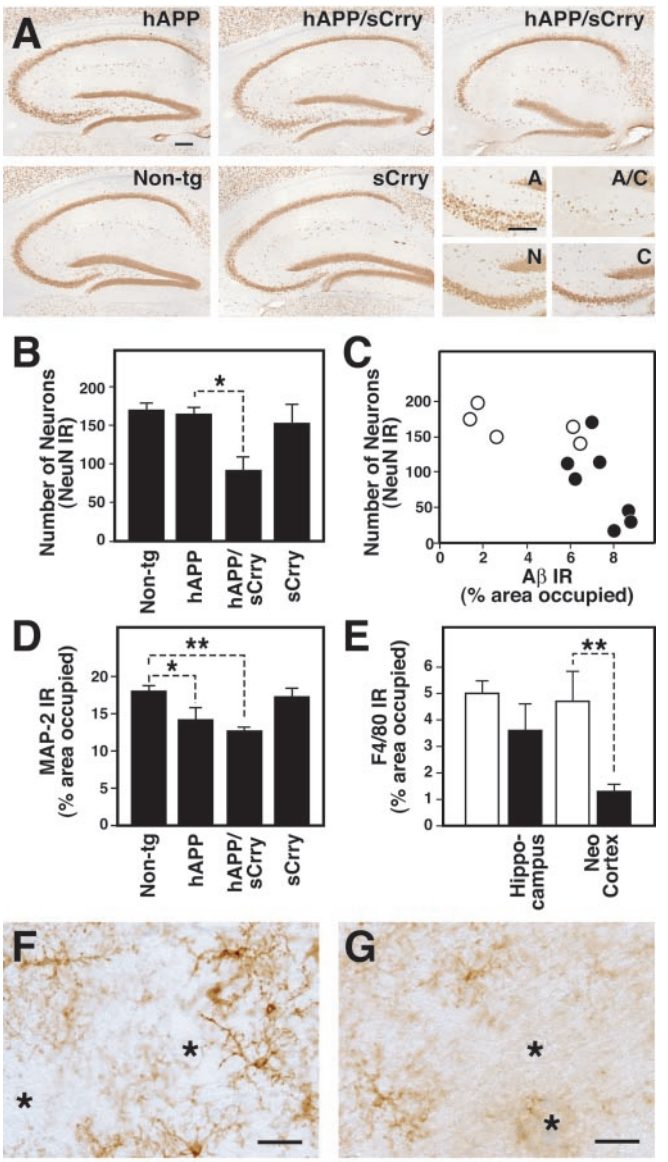

Fig. 4. Prominent neurodegeneration and reduced microgliosis in hAPP/sCrry mice. Brain sections from 10- to 12-month-old mice from a cross of hAPP with sCrry mice were analyzed for neurodegeneration and microglial activation. (*A*) NeuN immunostaining of 40-μm brain sections showed a prominent decrease in staining in the hippocampal CA3 region in hAPP/sCrry compared with single transgenic or nontransgenic (Non-tg) mice. The four panels in the bottom right corner show the CA3c subregion of the hAPP (A), sCrry (C), Non-tg (N), and the hAPP/sCrry (A/C) mouse in the upper right corner at higher magnification. (*B*) The number of NeuN-immunoreactive (IR) neurons in the CA2/CA3 region of the hippocampus was strongly reduced in hAPP/sCrry mice compared with littermate controls. Bars represent mean ± SEM from three sections per mouse and 5–8 mice per genotype. *, $P < 0.05$ by Tukey–Kramer test. (*C*) Relative numbers of NeuN-positive neurons in the CA2/CA3 region of the hippocampus of hAPP (○) and hAPP/sCrry (●) mice plotted against the percent area occupied by Aβ immunoreactive deposits (3D6 antibody). (*D*) Dendritic integrity determined as percent area occupied by MAP-2 immunoreactive dendrites in the stratum radiatum of the CA3 subfield of the hippocampus was reduced in hAPP and hAPP/sCrry mice. Bars represent mean ± SEM from 5–8 mice per genotype. *, $P < 0.05$; **, $P < 0.01$ by Tukey–Kramer test. (*E*) Microglial activation determined as the relative area of F4/80 immunoreactive products in the hippocampus or the midfrontal cortex was reduced in hAPP/sCrry (black bars) compared with hAPP (white bars) mice. Bars are mean ± SEM from 5–8 mice per group. **, $P = 0.008$ by *t* test. (*F* and *G*) Microglia surrounding amyloid plaques (indicated by asterisks) appear more activated and express more F4/80 immunoreactivity in hAPP (*F*) than in hAPP/sCrry (*G*) mice. [Scale bars: 100 μm (*A*), 20 μm (*F* and *G*).]

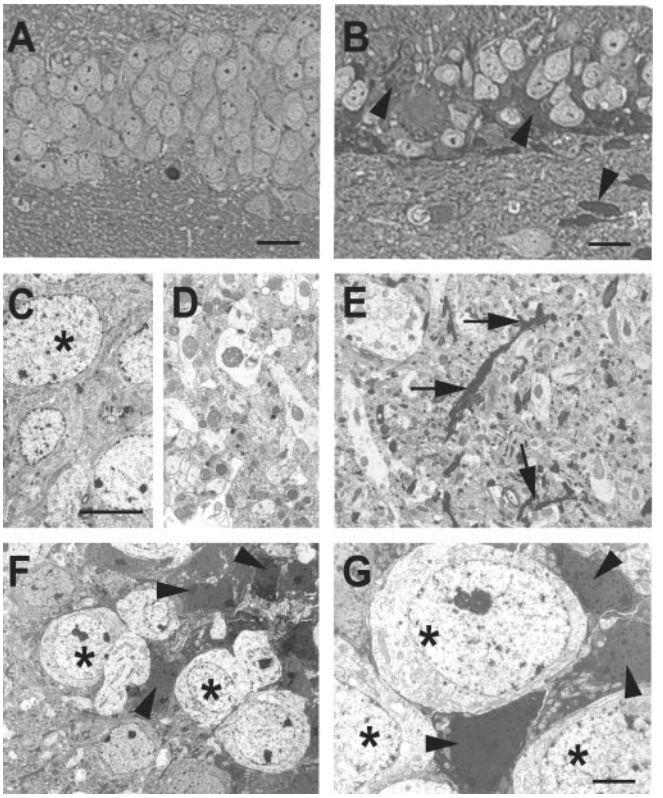

Fig. 5. Accumulation of degenerating neurons in hAPP/sCrry mice. Brain sections from 12-month-old nontransgenic (*A*, *C*, and *D*) or hAPP/sCrry mice (*B* and *E–G*) were stained with toluidine blue and viewed by light microscopy (*A* and *B*) or analyzed by electron microscopy (*C–G*). (*A* and *B*) Dentate gyrus of a nontransgenic (*A*) or hAPP/sCrry mouse (*B*) with darkly stained degenerating cells (arrow heads). (*C* and *D*) Normal appearing neurons (asterisks) in the dentate gyrus (*C*) and neuropil (*D*) in the hippocampal CA3 region of a nontransgenic mouse. (*E*) Degenerating neurites (arrows) in the CA3 region of the hippocampus in a hAPP/sCrry mouse. (*F* and *G*) Neurons with different degrees of electron density (arrow heads) indicating different degrees of degeneration in the dentate gyrus (*F*) or CA3 pyramidal layer (*G*). Asterisks mark healthy-appearing neurons. [Scale bars: 25 μm (*A* and *B*), 10 μm (*C–F*), 3 μm (*G*).]

amyloid and degenerating neurons. These findings provide evidence for a role of complement and innate immunity in AD-like disease in mice and support the concept that certain inflammatory defense mechanisms in the brain may be beneficial in neurodegenerative disease (2, 19, 36).

There is ample evidence that activated complement products accumulate in AD brains (reviewed in refs. 1 and 3) and in the brains of aged hAPP transgenic mice (37), and it is likely that the characteristic lesions of AD directly activate the complement system. C1q and C3 activation products or the MAC colocalize with amyloid deposits and degenerating, tangle-bearing neurons (1, 3), and complement was activated *in vitro* by fibrillar Aβ (20–22, 24) and isolated preparations of tangles from human brains (38). Interestingly, overexpression of sCrry in 3-month-old hAPP/sCrry mice led to a relative increase in Aβ_{1-42} (Fig. 2*G*), which is more fibrillogenic and a more potent activator of complement than Aβ_{1-40} *in vitro* (21, 22). It is conceivable that this selective increase is because of decreased complement activation in hAPP/sCrry mice and, as a result, a decrease in clearance of Aβ_{1-42}. Besides activation by aggregated proteins, complement may be activated by degenerating neurons or synapses and dying cells. For example, experimental nerve transections result in deposition of complement C1q and C3 on degenerating nerve terminals (39), and degenerating or dying cells in peripheral organs are decorated with complement activation products (40).

To prevent uncontrolled activation of complement at the cell surface and self-destruction, cells throughout the body express complement-regulatory proteins. Crry is one such protein that fulfills a key function in the mouse. Lack of Crry expression results in embryonic lethality, apparently because of sustained complement activation at the fetal-maternal interface (41). Conversely, transgenic overproduction of soluble Crry protected against antibody-induced complement attack and glomerular injury in the kidney (27, 33), and overexpression of sCrry in astrocytes of transgenic mice reduced immune-mediated CNS disease (32). Based on these findings and our immunohistochemical analysis of C3d expression in the hippocampus of hAPP and hAPP/sCrry mice, it is likely that the effects of sCrry observed in the current study relate to its complement inhibitory function. Other, yet unidentified functions of sCrry in the CNS may permit alternative explanations for our findings, including direct interactions of sCrry with Aβ, neurotoxic effects, or inhibitory effects on phagocytosis.

Recently, vaccination of hAPP mice with synthetic Aβ (8) reduced Aβ accumulation or cleared existing deposits in the brain and reversed cognitive deficits (6, 7). Although antibody receptor-mediated phagocytosis via microglia has been suggested to be the mechanism of clearance (9), antigen–antibody complexes (e.g., Aβ fibrils–Aβ antibody) are one of the most potent activators of the classical complement pathway (16), and our results suggest that complement facilitates or potentiates clearance in Aβ-vaccinated mice. Moreover, whereas antibody-mediated clearance of Aβ is an effective means to treat hAPP mice, complement-mediated clearance may be a natural way to rid the brain of accumulating Aβ fibrils. Our observations that hAPP/sCrry mice have increased Aβ deposition and reduced microglial activation, whereas hAPP/TGF-β1 mice have reduced Aβ deposition and increased microglial activation (13), provide additional support for a role of complement and microglia in Aβ clearance.

What is the function of complement in AD? Many have argued that the presence of complement activation products in the brain, and of the MAC on degenerating neurons in particular, indicates a detrimental role in AD (1–3). Consistent with a potentially detrimental role of complement in the CNS, genetic inhibition of complement in transgenic mice with astroglial overproduction of sCrry prevented experimental allergic encephalomyelitis or decreased its severity when compared with that in nontransgenic littermate controls (32). However, lack of C3 expression in C3 knockout mice increased disease severity 2-fold in the same experimental paradigm (42). Similarly, the complement activation products C3a and C5a were neuroprotective, and sublytic concentrations of the MAC protected oligodendrocytes and Schwann cells from apoptosis (reviewed in refs. 43 and 44). In addition, naturally C5-deficient mice were more susceptible to excitotoxic lesions than wild-type littermate controls (45). The findings of the current study also support a beneficial and possibly neuroprotective role of complement in mice overproducing hAPP/Aβ. In addition to direct neuroprotective effects (43, 44), complement may stimulate clearance and reduce the accumulation of Aβ and degenerating neurons via complement receptors on phagocytic microglia. A better understanding of complement in the brain may help to devise strategies to reduce Aβ and neuronal degeneration in AD as well.

We thank Lennart Mucke for helpful comments on the manuscript, Hilda Ordanza for help with mouse husbandry, Kelley Nelson for secretarial assistance, and Gary Howard and Stephen Ordway for editing of the manuscript. This work was supported by National Institutes of Health Grants AG15871 (to T.W.-C.), AI30040 (to J.D.L.), DK41873 and DK58820 (to R.J.Q.), and AG10869 and AG5131 (to E.M.), and by California Alzheimer's Disease Program Grant 98-15724 (to T.W.-C.).

1. Akiyama, H., Barger, S., Barnum, S., Bradt, B., Bauer, J., Cole, G. M., Cooper, N. R., Eikelenboom, P., Emmerling, M., Fiebich, B. L., *et al.* (2000) *Neurobiol. Aging* **21,** 383–421.
2. Wyss-Coray, T. & Mucke, L. (2002) *Neuron*, in press.
3. McGeer, P. L. & McGeer, E. G. (1999) *J. Leukocyte Biol.* **65,** 409–415.
4. Terry, R. D., Masliah, E. & Hansen, L. A. (1994) in *Alzheimer Disease*, eds. Terry, R. D., Katzman, R. & Bick, K. L. (Raven, New York), pp. 179–196.
5. Selkoe, D. J. (1999) *Nature (London)* **399,** A23–A31.
6. Morgan, D., Diamond, D. M., Gottschall, P. E., Ugen, K. E., Dickey, C., Hardy, J., Duff, K., Jantzen, P., DiCarlo, G., Wilcock, D., *et al.* (2000) *Nature (London)* **408,** 982–985.
7. Janus, C., Pearson, J., McLaurin, J., Mathews, P. M., Jiang, Y., Schmidt, S. D., Chishti, M. A., Horne, P., Heslin, D., French, J., *et al.* (2000) *Nature (London)* **408,** 979–982.
8. Schenk, D., Barbour, R., Dunn, W., Gordon, G., Grajeda, H., Guido, T., Hu, K., Huang, J., Johnson-Wood, K., Khan, K., *et al.* (1999) *Nature (London)* **400,** 173–177.
9. Bard, F., Cannon, C., Barbour, R., Burke, R., Games, D., Grajeda, H., Guido, T., Hu, K., Huang, J., Johnson-Wood, K., *et al.* (2000) *Nat. Med.* **6,** 916–919.
10. Bacskai, B. J., Kajdasz, S. T., Christie, R. H., Carter, C., Games, D., Seubert, P., Schenk, D. & Hyman, B. T. (2001) *Nat. Med.* **7,** 369–372.
11. Frautschy, S. A., Cole, G. M. & Baird, A. (1992) *Am. J. Pathol.* **140,** 1389–1399.
12. Jantzen, P. T., Connor, K. E., DiCarlo, G., Wenk, G. L., Wallace, J. L., Rojani, A. M., Coppola, D., Morgan, D. & Gordon, M. N. (2002) *J. Neurosci.* **22,** 2246–2254.
13. Wyss-Coray, T., Lin, C., Yan, F., Yu, G., Rohde, M., McConlogue, L., Masliah, E. & Mucke, L. (2001) *Nat. Med.* **7,** 614–618.
14. Giulian, D. (1999) *Am. J. Hum. Genet.* **65,** 13–18.
15. Song, W.-C., Sarrias, M. R. & Lambris, J. D. (2000) *Immunopharmacology* **49,** 187–198.
16. Holers, V. M. (1996) in *Clinical Immunology: Principles and Practice,* ed. Rich, R. R. (Mosby, St. Louis), pp. 363–391.
17. Rogers, J., Webster, S., Lue, L. F., Brachova, L., Civin, W. H., Emmerling, M., Shivers, B., Walker, D. & McGeer, P. (1996) *Neurobiol. Aging* **17,** 681–686.
18. Emmerling, M. R., Watson, M. D., Raby, C. A. & Spiegel, K. (2000) *Biochim. Biophys. Acta* **1502,** 158–171.
19. Gasque, P., Dean, Y. D., McGreal, E. P., Beek, J. V. & Morgan, B. P. (2000) *Immunopharmacology* **49,** 171–186.
20. Rogers, J., Cooper, N. R., Webster, S., Schultz, J., McGeer, P. L., Styren, S. D., Civin, W. H., Brachova, L., Bradt, B., Ward, P. & Lieberburg, I. (1992) *Proc. Natl. Acad. Sci. USA* **89,** 10016–10020.
21. Jiang, H., Burdick, D., Glabe, C. G., Cotman, C. W. & Tenner, A. J. (1994) *J. Immunol.* **152,** 5050–5059.
22. Watson, M. D., Roher, A. E., Kim, K. S., Spiegel, K. & Emmerling, M. R. (1997) *Amyloid* **4,** 147–156.
23. Webster, S., Bradt, B., Rogers, J. & Cooper, N. (1997) *J. Neurochem.* **69,** 388–398.
24. Bradt, B. M., Kolb, W. P. & Cooper, N. R. (1998) *J. Exp. Med.* **188,** 431–438.
25. Sahu, A. & Lambris, J. (2001) *Immunol. Rev.* **180,** 35–48.
26. Molina, H., Wong, W., Kinoshita, T., Brenner, C., Foley, S. & Holers, V. M. (1992) *J. Exp. Med.* **175,** 121–129.
27. Quigg, R. J., He, C., Lim, A., Berthiaume, D., Alexander, J. J., Kraus, D. & Holers, V. M. (1998) *J. Exp. Med.* **188,** 1321–1331.
28. Mucke, L., Masliah, E., Yu, G.-Q., Mallory, M., Rockenstein, E. M., Tatsuno, G., Hu, K., Kholodenko, D., Johnson-Wood, K. & McConlogue, L. (2000) *J. Neurosci.* **20,** 4050–4058.
29. Mucke, L., Masliah, E., Johnson, W. B., Ruppe, M. D., Alford, M., Rockenstein, E. M., Forss-Petter, S., Pietropaolo, M., Mallory, M. & Abraham, C. R. (1994) *Brain Res.* **666,** 151–167.
30. Abusaad, I., MacKay, D., Zhao, J., Stanford, P., Collier, D. A. & Everall, I. P. (1999) *J. Comp. Neurol.* **408,** 560–566.
31. Johnson-Wood, K., Lee, M., Motter, R., Hu, K., Gordon, G., Barbour, R., Khan, K., Gordon, M., Tan, H., Games, D., *et al.* (1997) *Proc. Natl. Acad. Sci. USA* **94,** 1550–1555.
32. Davoust, N., Nataf, S., Reiman, R., Holers, M. V., Campbell, I. L. & Barnum, S. R. (1999) *J. Immunol.* **163,** 6551–6556.
33. Alexander, J. J., Lim, A., He, R. L., MacDonald, R. L., Holers, V. M. & Quigg, R. J. (1999) *Immunopharmacology* **42,** 245–254.
34. Mullen, R. J., Buck, C. R. & Smith, A. M. (1992) *Development (Cambridge, U.K.)* **116,** 201–211.
35. Larsson, E., Lindvall, O. & Kokaia, Z. (2001) *Brain Res.* **913,** 117–132.
36. Abraham, C. R. (2001) *Neurbiol. Aging* **22,** 931–936.
37. Matsuoka, Y., Picciano, M., Malester, B., LaFrancois, J., Zehr, C., Daeschner, J. M., Olschowka, J. A., Fonseca, M. I., O'Banion, M. K., Tenner, A. J., *et al.* (2001) *Am. J. Pathol.* **158,** 1345–1354.
38. Shen, Y., Lue, L.-F., Yang, L.-B., Roher, A., Kuo, Y.-M., Strohhmeyer, R., Goux, W. J., Lee, V., Johnson, G. V. W., Webster, S. D., *et al.* (2001) *Neurosci. Lett.* **305,** 165–168.
39. Aldskogius, H., Liu, L. & Svensson, M. (1999) *J. Neurosci. Res.* **58,** 33–41.
40. Botto, M., Dell'Agnola, C., Bygrave, A. E., Thompson, E. M., Cook, H. T., Petry, F., Loos, M., Pandolfi, P. P. & Walport, M. J. (1998) *Nat. Genet.* **19,** 56–59.
41. Xu, C., Mao, D., Holers, V. M., Palanca, B., Cheng, A. M. & Molina, H. (2000) *Science* **287,** 498–501.
42. Calida, D. M., Constantinescu, C., Purev, E., Zhang, G.-X., Ventura, E. S., Lavi, E. & Rostami, A. (2001) *J. Immunol.* **166,** 723–726.
43. Nataf, S., Stahel, P. F., Davoust, N. & Barnum, S. R. (1999) *Trends Neurosci.* **22,** 397–402.
44. Fishelson, Z., Attali, G. & Mevorach, D. (2001) *Mol. Immunol.* **38,** 207–219.
45. Pasinetti, G. M., Tocco, G., Sakhi, S., Musleh, W. D., DeSimoni, M. G., Pascarucci, P., Schreiber, S., Baudry, M. & Finch, C. E. (1996) *Neurobiol. Dis.* **3,** 197–204.